

# High-Throughput Exploration of NV-like Color Centers Across Host Materials

Oscar Groppfeldt,<sup>\*</sup> Joel Davidsson,<sup>†</sup> and Rickard Armiento<sup>‡</sup>

*Department of Physics, Chemistry and Biology, Linköping University, Linköping, Sweden*

Point defects in semiconductors offer a promising platform for advancing quantum technologies due to their localized energy states and controllable spin properties. Prior research has focused on a limited set of defects within materials such as diamond, silicon carbide, and hexagonal boron nitride. We present a high-throughput study to systematically identify and evaluate point defects across a diverse range of host materials, aiming to uncover previously unexplored defects in novel host materials suitable for use in quantum applications. A range of host materials are selected for their desirable properties, such as appropriate bandgaps, crystal structure, and absence of d- or f-electrons. The Automatic Defect Analysis and Qualification (ADAQ) software framework is used to generate vacancies, substitutions with s- and p-elements, and interstitials in these materials and use density functional theory to calculate key properties such as Zero-Phonon Lines (ZPLs), ionic displacements, Transition Dipole Moments (TDMs), and formation energies. Special attention is given to charge correction methods for materials with dielectric anisotropy. We uncover new defect-host combinations with advantageous properties for quantum applications: 28 defects across 11 isotropic and 2 anisotropic host materials show properties similar to the nitrogen-vacancy (NV) center in diamond. Beryllium (Be) substitutional defects in SrS, MgS, and SrO emerge as particularly promising. These findings contribute to diversifying and enhancing the materials available for quantum technologies.

## I. INTRODUCTION

The potential of quantum technologies to revolutionize fields such as computing, cryptography, and sensing, drive the need for stable physical systems capable of supporting these advancements. Among various candidates, point defects in semiconductors with localized energy states due to atomic imperfections provide a promising platform for quantum applications [1, 2].

Quantum applications require systems with specific physical characteristics, such as stable spin states and controllable optical transitions, to enable applications like quantum computing, communication, and sensing. Point defects in semiconductors have emerged as one such system, with defects like the nitrogen-vacancy (NV) center in diamond [3–5] already being fundamental components of various quantum devices and applications. However, as the number of applications of these technologies grows, so does the need for alternative host materials and defect configurations [6]. With this growing demand, it is important to understand the fundamental properties that make point defects viable for quantum applications. By examining the characteristics, we can identify new defect systems and configurations that meet the criteria of emerging technologies.

Weber *et al.* lists five critical characteristics needed to ensure point defects are stable and efficient when participating in quantum operations as qubits [7]. They need to (*i*) be long-lived bound states with spin sublevels; (*ii*) allow optical pumping for state polarization; (*iii*) have

sublevel-dependent luminescence; (*iv*) have interference-free optical transitions; and (*v*) their bound states must have thermal stability. This list was derived from the properties observed for the nitrogen-vacancy (NV) center in diamond, the predominant defect for quantum applications.

The potential of systematic high-throughput methods to identify promising candidates for quantum applications have been demonstrated by recent studies on point defects in 2D and 3D materials. Highlights include, e.g., several studies on materials like diamond [8, 9], silicon [10–12], hexagonal boron nitride [13–15], and tungsten disulfide [16]. These kinds of studies not only uncover defects with remarkable capabilities to characterize in more detail, but also provide quantitative insight into trends of defects in the materials. However, the narrow focus on rather few host materials may limit the discovery of defect systems in other hosts with advantages for specific applications. Some prior works have targeted this gap for 2D host materials. For example, Bertoldo *et al.* examined 1900 defects in 82 different 2D semiconductors and insulators [17]. In a similar study, Huang *et al.* produced a database with over 11,000 defect configurations across six 2D materials [18]. These studies have resulted in large databases of defect configurations in 2D materials. The authors are not aware of a database with defect data over a similar range of bulk host materials. To discover novel defect systems in less explored host materials with properties appropriate for next-generation quantum technologies will pave the way for advancements in quantum computing, secure communication, and precision sensing.

In this work, we aim to address the lack of known point defects with interesting properties in less studied materials by a systematic high-throughput study across a wide range of host materials. We screen all single point de-

---

<sup>\*</sup> oscar.groppfeldt@liu.se

<sup>†</sup> joel.davidsson@liu.se

<sup>‡</sup> rickard.armiento@liu.se

fects consisting of substitutional and interstitial s- and p-elements, as well as vacancies in thirteen host materials selected from a list of suitable materials for hosting quantum defects compiled by Ferrenti *et al.* [19]. This list was further narrowed down based on symmetry, band gaps and stability to 32 materials (see Sec. III). The screening is performed using the Automatic Defect Analysis and Qualification (ADAQ) software framework [20] implemented using the high-throughput toolkit (*httk*) [21], to generate the defect systems and accurately calculate their magneto-optical properties. ADAQ has previously been successfully used to discover interesting defects in SiC [22], CaO [23], diamond [9], and MgO [24].

## II. DEFECT PROPERTIES

Essential properties of defects that determine their viability for quantum information applications are presented in the following subsections.

### A. Zero-phonon Line (ZPL)

A key property for quantum applications is the ability of a defect to emit photons at specific wavelengths. This ability stems from the zero-phonon line, where no phonon interactions occur during the relaxation from the excited state to the ground state. Without any interactions from surrounding phonons, the emitted photon carries the entire energy difference between the states, ensuring that the photon has the same wavelength every time it is emitted in the ZPL. The ZPL is given by

$$E_{\text{ZPL}} = E_{e,\text{min}} - E_{g,\text{min}}, \quad (1)$$

where  $E_{g,\text{min}}$  and  $E_{e,\text{min}}$  are the energies of the ground and excited states.

### B. Huang-Rhys factor

The Huang-Rhys factor  $S$  quantifies the coupling between electronic states and vibrational modes [25]. Defects with lower Huang-Rhys factors exhibit minimal vibrational losses, increasing the probability that an emission occurs through the ZPL. The Huang-Rhys factor is expensive to calculate, but it can be estimated using the following 1D model (one-phonon approximation):

$$S = \sum_k S_k, \quad \text{with} \quad (2)$$

$$S_k = \frac{\omega_k q_k^2}{2\hbar}, \quad \text{and} \quad (3)$$

$$q_k^2 = \sum_i m_i |R_{e_i} - R_{g_i}|. \quad (4)$$

Here,  $k$  indexes the phonon mode with frequency  $\omega_k$  and  $q_k$  is the sum of ionic displacements between the excited

state  $e_i$  and ground state  $g_i$  over all ions  $i$  with weight  $m_i$  [20, 26]. As the estimated Huang-Rhys factor is calculated using  $\Delta Q$ , it is reported instead of the Huang-Rhys factor.

### C. Transition Dipole Moment (TDM)

As an electron absorbs a photon, it transitions from its ground state  $|\psi_g\rangle$  to an excited state  $|\psi_e\rangle$ . The probability of the specific transition  $|\psi_g\rangle \rightarrow |\psi_e\rangle$  is given by the associated transition dipole moment  $\mu_{ge}$ . Using the Born-Oppenheimer approximation [27], the TDM is given by

$$\hat{\mu} = \langle \psi_g | q \hat{r} | \psi_e \rangle = \frac{i\hbar}{(\varepsilon_e - \varepsilon_g)m} \langle \psi_e | \hat{p} | \psi_g \rangle, \quad (5)$$

where  $\varepsilon_i$  is the energy of state  $i$ . The TDM is of particular interest as it directly relates to the intensity of the ZPL. The wavefunctions  $|\psi_e\rangle$  and  $|\psi_g\rangle$  are taken from the WAVECARs produced by VASP for the excited state and ground state calculations, respectively [28].

### D. Formation energy

The energy required for a defect to form is given by its formation energy  $\Delta H_{D,q}$ . It is calculated as

$$\Delta H_{D,q}(E_f, \mu) = (E_{D,q} - E_H) + \sum_i n_i \mu_i + qE_f + E_{\text{corr}}(q) \quad (6)$$

for a defect with charge  $q$ . Here,  $E_{D,q} - E_H$  is the difference in energy between the system containing the defect and the host,  $E_f$  is the Fermi energy, and the sum runs over all atomic species  $i$  that have been removed ( $n_i > 0$ ) or added ( $n_i < 0$ ), scaled by their chemical potential  $\mu_i$ . Furthermore,  $E_{\text{corr}}$  is a correction for the error in energy arising from the periodic boundary conditions used in the DFT calculations. In this study, the charge correction by Kumagai and Oba [29] is used. The expression for the charge correction potential can be found in Eq. (7).

$$V_q^{\text{aniso}} = \sum_{\mathbf{R}_i}^{i \neq 0} \frac{q}{\sqrt{|\bar{\varepsilon}|}} \frac{\text{erfc}(\gamma \sqrt{\mathbf{R}_i \cdot \bar{\varepsilon}^{-1} \cdot \mathbf{R}_i})}{\sqrt{\mathbf{R}_i \cdot \bar{\varepsilon}^{-1} \cdot \mathbf{R}_i}} - \frac{\pi q}{\Omega \gamma^2} + \sum_{\mathbf{G}_i}^{i \neq 0} \frac{4\pi q}{\Omega} \frac{\exp(-\mathbf{G}_i \cdot \bar{\varepsilon} \cdot \mathbf{G}_i / 4\gamma^2)}{\mathbf{G}_i \cdot \bar{\varepsilon} \cdot \mathbf{G}_i} - \frac{2\gamma q}{\sqrt{\pi |\bar{\varepsilon}|}}. \quad (7)$$

This potential then gives the charge correction energy  $E_q^{\text{corr}}$  by scaling with half the charge  $q$ ;  $E_q^{\text{corr}} = \frac{q}{2} V_q^{\text{aniso}}$ .

### E. Defect hull

The defect hull is spanned by the defects with the lowest formation energy in each stoichiometry as a function

Host	mp-id	Space group	T2 (s) [31]
CaS	mp-1672	225	0.02250206
CaCO3	mp-3953	167	0.010523766
SrS	mp-1087	225	0.002386663
CaSe	mp-1415	225	0.001984719
SrSe	mp-2758	225	0.001767484
BaS3	mp-239	113	0.00172218
SrO	mp-2472	225	0.001515751
SrTe	mp-1958	225	0.001226839
MgS	mp-1315	225	0.001156499
BaSe	mp-1253	225	0.001143197
BaS	mp-1500	225	0.001127442
BaTe	mp-1000	225	0.001075876
BaO	mp-1342	225	0.000741652

TABLE I. The selected host materials along with their identifier in the materials project database, and calculated T2 time.

of the Fermi level. Defects on the defect hull are considered thermodynamically stable relative to other defects of the same stoichiometric composition. The defect hull has successfully been leveraged to predict new defects in 4H-SiC, which were identified experimentally [22].

### III. HOST MATERIAL SELECTION AND DEFECT GENERATION

The starting point for selecting the host materials to investigate in this work is a list of Ferrenti *et al.* [19] that identified 541 materials from the materials project database [30] as particularly suitable for hosting quantum defects. From this list we select all (*i*) single crystal materials (*ii*) on the convex hull of thermodynamical stability (*iii*) without d- or f-elements, (*iv*) a band gap of 1.0 eV or more, which (*v*) has not previously investigated using ADAQ. Furthermore, we also (*vi*) remove materials with a space group number below 75 to focus on materials with symmetries that support the kind of degeneracy that can give NV-like spin-1 defects; for these space groups the crystallographic point group has only 1-dimensional irreps, which has no states with symmetry enforced essential degeneracy. The remaining materials are sorted by their quantum coherence times as calculated in Ref. 31. As a final step we manually select 11 isotropic and 2 anisotropic materials from this list with compositions and structural complexity appropriate for our methods. The crystal structures are obtained using the Materials Project API [30]. Details on the resulting host materials are presented in Table I.

For each host, we generate a set of single point defects, including vacancies, substitutionals, and interstitials. The generation is limited by a number of constraints: (*i*) *Spatial constraints*: the minimum lattice parameter length is taken to be 20 Å to ensure that the generated defects are well separated spatially and single-point defects are generated individually, with no clusters or extended defects; (*ii*) *Substitutional constraints*: dopand species are only allowed to be intrinsic or ele-

ments from the s- and p-blocks of the periodic table; (*iii*) *Interstitial placement constraints*: distances between interstitial atoms and surrounding host atoms are restricted to a range of 1 Å to 3.5 Å.

### IV. COMPUTATIONAL DETAILS

We use the ADAQ framework [20] implemented using the high-throughput toolkit (*httk*) [21] to generate defects, run automated workflows for ab initio simulations, calculate relevant properties, and identify defects of interest. The ab initio calculations uses the Vienna Ab initio Simulation Package (VASP) [32] using the exchange-correlation functional by Perdew, Burke and Ernzerhof (PBE) [33]. The convergence settings for screening-level ADAQ calculations from Ref. [20] were used. These convergence settings include a plane wave energy cutoff of 600 eV and a kinetic energy cutoff of 900 eV, which are chosen to cover the requirements of a wide range of elements. In addition, the Fast Fourier Transform (FFT) grid is set to twice the largest wave vector, and a  $\Gamma$ -centered Monkhost-Pack k-point grid is used. When performing calculations at the  $\Gamma$ -point only, Fermi smearing with a width of 1 meV is applied. For defect calculations, no symmetry is applied.

### V. RESULTS

As described above, point defects in 11 isotropic and 2 anisotropic host materials were investigated for key properties such as ZPL energies, TDM values, and defect stability. The host materials investigated and their Materials Project IDs are shown in Table III. For each of the isotropic materials in the table, 175 defects were evaluated. For the anisotropic materials, CaCO3 and BaS3, 1085 and 1540 defects were evaluated, respectively.

Among the isotropic materials studied, we identify 28 NV-like defects across 10 of the host materials (BaTe, BaS3, and SrTe did not have any NV-like defects), all of them are on the defect hull with spin 1, except the  $\text{Te}_{\text{Sr}}$  in SrO which has spin  $\frac{3}{2}$ . These NV-like defects are listed in Table II. A key highlight from the isotropic host materials is the beryllium substitutionals, which appears in three different host materials MgS, SrS, and SrO. The formation energies for these substitutionals are shown in Figure 1, 2, and 3, respectively. For the anisotropic hosts, a single NV-like defect was identified in CaCO3; a hydrogen substitutional  $\text{H}_{\text{C}}$  with charge  $-1$  and spin 1. The ZPL was 0.54 eV with a TDM of 12.93 Debye. The related  $\Delta Q$  was 1.15.

### VI. DISCUSSION

It is apparent in Table II that there is a large representation of NV-like defects in SrO, with 11 out of 28 defects

TABLE II: Defect systems with a converged ZPL  $> 0.5$  eV, spin 1, a TDM larger than 3 Debye, and on the defect hull.

Host	Defect type	Charge	ZPL (eV)	TDM (Debye)	$\Delta Q$ (amu <sup>1/2</sup> )
BaS	Int <sub>P</sub>	1	1.04	7.37	4.45
	Be <sub>S</sub>	0	2.06	8.22	0.55
SrS	Int <sub>Ge</sub>	0	1.44	3.9	2.06
	Int <sub>Si</sub>	0	1.07	4.95	1.95
CaS	Int <sub>Si</sub>	0	1.05	5.15	1.46
SrSe	Int <sub>Ge</sub>	0	1.38	3.37	2.41
MgS	Be <sub>S</sub>	0	1.94	9.22	0.65
SrO	Te <sub>Sr</sub> *	-1	1.91	10.0	1.76
	Be <sub>O</sub>	0	1.95	8.51	0.67
	Int <sub>C</sub>	0	1.29	7.16	1.98
	As <sub>Sr</sub>	-1	2.44	9.21	1.75
	Int <sub>Pb</sub>	0	2.13	4.94	1.41
	I <sub>Sr</sub>	-1	1.17	3.98	1.83
	Int <sub>Sn</sub>	0	1.77	7.3	1.36
	Int <sub>Ge</sub>	0	1.79	6.8	1.58
	Int <sub>Sb</sub>	1	1.62	5.44	0.69
	P <sub>Sr</sub>	-1	2.28	11.81	2.09
BaO	Int <sub>As</sub>	1	1.47	8.42	1.59
	Int <sub>Sb</sub>	1	1.0	8.07	2.46
BaSe	Int <sub>P</sub>	1	1.08	7.86	1.9
	Int <sub>Si</sub>	0	0.92	4.17	3.27
	Int <sub>Sb</sub>	1	0.88	5.97	10.02
	Int <sub>Ge</sub>	0	1.2	3.13	3.32
CaSe	Int <sub>Sn</sub>	0	1.17	4.04	2.79
	Int <sub>Ge</sub>	0	1.25	3.63	1.6
	Int <sub>Sn</sub>	0	1.21	4.17	1.57
CaCO3	Int <sub>Si</sub>	0	0.99	4.07	1.48
	H <sub>C</sub>	-1	0.54	12.93	1.15

\*spin-3/2

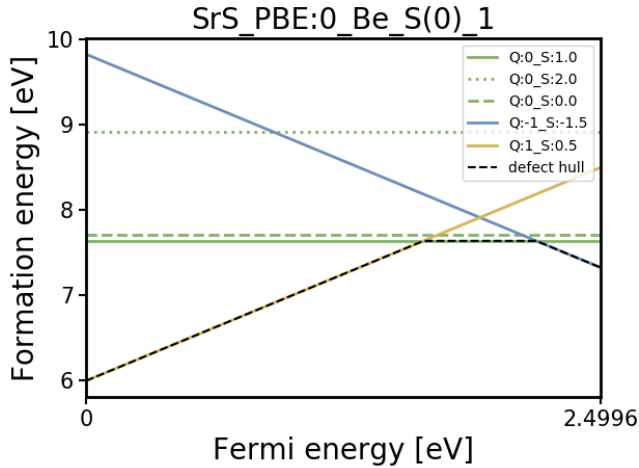


FIG. 1. Formation energy for Be<sub>S</sub> in SrS.

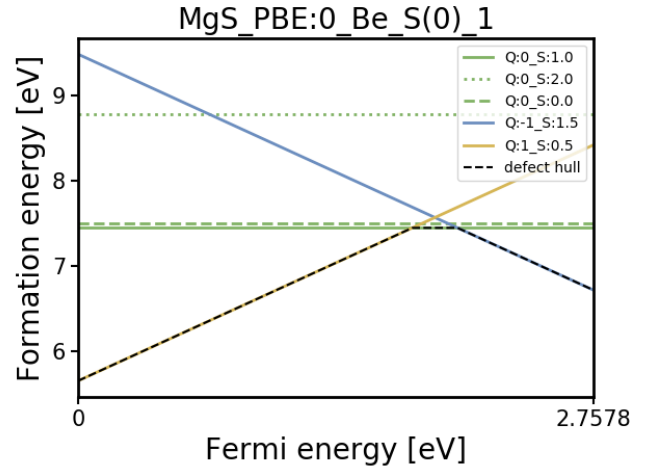


FIG. 2. Formation energy for Be<sub>S</sub> in MgS.

identified residing in this host material. These results suggest a future more in-depth study of SrO is motivated. Furthermore, beryllium occurs three times as a substitutional defect, all with similar properties. Their  $\Delta Q$  range from 0.55 to 0.67, which indicates that a large portion of

their emissions occur in the ZPL. The ZPLs also have a comparatively strong intensity, with the TDMs being between 8.22 and 9.22, with emissions estimated to be around 2 eV, placing them in the red part of the visible spectrum. While these wavelengths are too short for di-

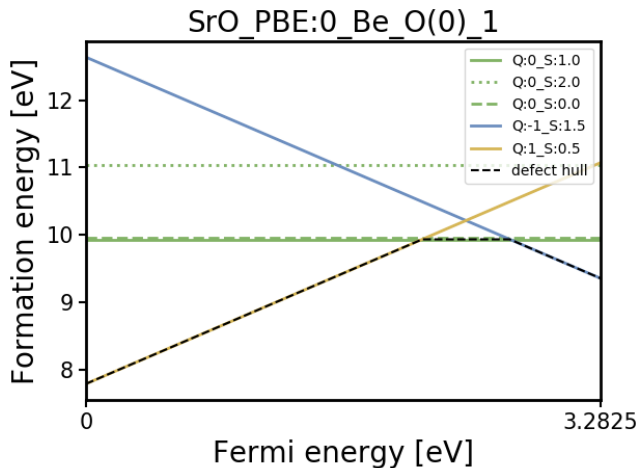


FIG. 3. Formation energy for  $\text{Be}_\text{O}$  in  $\text{SrO}$ .

rect use in current telecom optics, [34, 35] they are close to that of the emissions of the  $\text{NV}^-$  center. [26] This similarity is advantageous, as it may be possible to adopt methods for adapting the emissions of the  $\text{NV}^-$  center to interoperate with telecom wavelengths, which have already been successfully demonstrated to work [36]. While these beryllium substitutionals seem promising, note that the reported ZPL, TDM, and  $\Delta Q$  values are only calculated to screening-level accuracy. Further verification by more accurate methods, such as HSE06 [37], should be performed to validate their viability.

The small amounts of NV-like defects in the anisotropic materials is disappointing but not completely unexpected.  $\text{BaS}_3$  has space group 113 and  $\text{CaCO}_3$  has 167, both with distinctly lower symmetry than the space group 225 shared by all the isotropic materials. The symmetry of systems with defects are limited by the symmetry of the pure host material, and a less symmetric system

implies a less symmetric Hamiltonian. This, in turn, decreases the probability for degenerate states, which translates to a smaller chance for spin 1 defects. However, the one NV-like defect found in these materials, the  $\text{H}_\text{C}$  defect in  $\text{CaCO}_3$ , stands out with the highest TDM of all the identified defects, which suggests that the screening of anisotropic materials is nevertheless motivated.

In this study, we have only considered single point defects. In practice, defect clusters are commonly observed. [38]. In particular, vacancies are frequently sufficiently mobile to be able to migrate into more energetically favorable positions where they can combine with other defects to form larger clusters [39, 40]. Hence, a future extension of the present study to more complex defects seems motivated.

## VII. CONCLUSION

In this work, we have provided a systematic exploration of point defects for quantum technologies across 13 host materials. By leveraging high-throughput computational methods, using density functional theory and the ADAQ framework, several new and promising defect systems have been identified. Notably, substitutional beryllium defects in  $\text{SrS}$ ,  $\text{MgS}$ , and  $\text{SrO}$  emerge as particularly interesting due to their strong ZPL properties comparable to that of the well studied NV-center in diamond, and potentially offer improved photon emission characteristics. This study opens for future works with a focus on refining the understanding of these systems through more computationally intensive techniques and experimental validation. Additionally, extending the high-throughput approach to account for defect-vacancy pairs may prove fruitful in uncovering new candidates. By advancing the search for and characterization of such defects, this study contributes to the ongoing effort to diversify and enhance the material platforms available for quantum technologies.

- 
- [1] G. Zhang, Y. Cheng, J.-P. Chou, and A. Gali, Material platforms for defect qubits and single-photon emitters, *Applied Physics Reviews* **7**, 031308 (2020).
  - [2] D. D. Awschalom, R. Hanson, J. Wrachtrup, and B. B. Zhou, Quantum technologies with optically interfaced solid-state spins, *Nature Photonics* **12**, 516 (2018), publisher: Nature Publishing Group.
  - [3] G. Davies, M. F. Hamer, and W. C. Price, Optical studies of the 1.945 eV vibronic band in diamond, *Proc. R. Soc. A Math. Phys. Sci.* **348**, 285 (1976).
  - [4] A. Gali, Ab initio theory of the nitrogen-vacancy center in diamond, *Nanophotonics* **8**, 1907 (2019), publisher: De Gruyter.
  - [5] M. W. Doherty, N. B. Manson, P. Delaney, F. Jelezko, J. Wrachtrup, and L. C. L. Hollenberg, The nitrogen-vacancy colour centre in diamond, *Physics Reports* **528**, 1 (2013).
  - [6] G. Wolfowicz, F. J. Heremans, C. P. Anderson, S. Kanai, H. Seo, A. Gali, G. Galli, and D. D. Awschalom, Quantum guidelines for solid-state spin defects, *Nature Reviews Materials* **6**, 906 (2021), publisher: Nature Publishing Group.
  - [7] J. Weber, W. Koehl, J. Varley, A. Janotti, B. Buckley, C. Van de Walle, and D. D. Awschalom, Quantum computing with defects, *Proceedings of the National Academy of Sciences* **107**, 8513 (2010).
  - [8] T. Lühmann, N. Raatz, R. John, M. Lesik, J. Rödiger, D. Wildanger, F. Kleissler, K. Nordlund, A. Zaitsev, J.-F. Roch, *et al.*, Screening and engineering of colour centres in diamond, *Journal of Physics D: Applied Physics* **51**, 483002 (2018).
  - [9] J. Davidsson, W. Stenlund, A. S. Parackal, R. Armiento, and I. A. Abrikosov, Na in diamond: High spin defects revealed by the adaq high-throughput computational database, *npj Computational Materials* **10**, 109

- (2024).
- [10] Y. Xiong, C. Bourgois, N. Sheremetyeva, W. Chen, D. Dahliah, H. Song, J. Zheng, S. M. Griffin, A. Sipahigil, and G. Hautier, High-throughput identification of spin-photon interfaces in silicon, *Science Advances* **9**, eadh8617 (2023).
- [11] Y. Xiong, J. Zheng, S. McBride, X. Zhang, S. M. Griffin, and G. Hautier, Discovery of t center-like quantum defects in silicon, arXiv preprint arXiv:2405.05165 (2024).
- [12] V. Ivanov, A. Ivanov, J. Simoni, P. Parajuli, B. Kanté, T. Schenkel, and L. Tan, Database of semiconductor point-defect properties for applications in quantum technologies, arXiv preprint arXiv:2303.16283 (2023).
- [13] S. A. Tawfik, S. Ali, M. Fronzi, M. Kianinia, T. T. Tran, C. Stampfl, I. Aharonovich, M. Toth, and M. J. Ford, First-principles investigation of quantum emission from hbn defects, *Nanoscale* **9**, 13575 (2017).
- [14] S. Vaidya, X. Gao, S. Dikshit, I. Aharonovich, and T. Li, Quantum sensing and imaging with spin defects in hexagonal boron nitride, *Advances in Physics: X* **8**, 2206049 (2023).
- [15] C. Cholsuk, A. Zand, A. Çakan, and T. Vogl, The hbn defects database: a theoretical compilation of color centers in hexagonal boron nitride, *The Journal of Physical Chemistry C* **128**, 12716 (2024).
- [16] J. C. Thomas, W. Chen, Y. Xiong, B. A. Barker, J. Zhou, W. Chen, A. Rossi, N. Kelly, Z. Yu, D. Zhou, *et al.*, A substitutional quantum defect in ws<sub>2</sub> discovered by high-throughput computational screening and fabricated by site-selective stm manipulation, *Nature communications* **15**, 3556 (2024).
- [17] F. Bertoldo, S. Ali, S. Manti, and K. S. Thygesen, Quantum point defects in 2d materials-the qpod database, *npj Computational Materials* **8**, 56 (2022).
- [18] P. Huang, R. Lukin, M. Faleev, N. Kazeev, A. R. Al-Maeeni, D. V. Andreeva, A. Ustyuzhanin, A. Tormasov, A. Castro Neto, and K. S. Novoselov, Unveiling the complex structure-property correlation of defects in 2d materials based on high throughput datasets, *npj 2D Materials and Applications* **7**, 6 (2023).
- [19] A. M. Ferrenti, N. P. de Leon, J. D. Thompson, and R. J. Cava, Identifying candidate hosts for quantum defects via data mining, *npj Computational Materials* **6**, 126 (2020).
- [20] J. Davidsson, V. Ivády, R. Armiento, and I. A. Abrikosov, Adaq: automatic workflows for magneto-optical properties of point defects in semiconductors, *Computer Physics Communications* **269**, 108091 (2021).
- [21] R. Armiento, Database-driven high-throughput calculations and machine learning models for materials design, *Machine Learning Meets Quantum Physics* , 377 (2020).
- [22] J. Davidsson, R. Babar, D. Shafizadeh, I. G. Ivanov, V. Ivády, R. Armiento, and I. A. Abrikosov, Exhaustive characterization of modified si vacancies in 4h-sic, *Nanophotonics* **11**, 4565 (2022).
- [23] J. Davidsson, M. Onizhuk, C. Vorwerk, and G. Galli, Discovery of atomic clock-like spin defects in simple oxides from first principles, *Nature Communications* **15**, 4812 (2024).
- [24] V. Somjit, J. Davidsson, Y. Jin, and G. Galli, An nv-center in magnesium oxide as a spin qubit for hybrid quantum technologies, arXiv preprint arXiv:2409.00246 (2024).
- [25] K. Huang and A. Rhys, Theory of light absorption and non-radiative transitions in f-centres, *Proceedings of the Royal Society of London. Series A. Mathematical and Physical Sciences* **204**, 406 (1950).
- [26] A. Alkauskas, B. B. Buckley, D. D. Awschalom, and C. G. Van de Walle, First-principles theory of the luminescence lineshape for the triplet transition in diamond nv centres, *New Journal of Physics* **16**, 073026 (2014).
- [27] J. Oppenheimer and M. Born, Zur quantentheorie der moleküle, *Ann Phys (Leipzig)* (1927).
- [28] J. Davidsson, Theoretical polarization of zero phonon lines in point defects, *Journal of Physics: Condensed Matter* **32**, 385502 (2020).
- [29] Y. Kumagai and F. Oba, Electrostatics-based finite-size corrections for first-principles point defect calculations, *Physical Review B* **89**, 195205 (2014).
- [30] A. Jain, S. P. Ong, G. Hautier, W. Chen, W. D. Richards, S. Dacek, S. Cholia, D. Gunter, D. Skinner, G. Ceder, *et al.*, Commentary: The materials project: A materials genome approach to accelerating materials innovation, *APL materials* **1** (2013).
- [31] S. Kanai, F. J. Heremans, H. Seo, G. Wolfowicz, C. P. Anderson, S. E. Sullivan, M. Onizhuk, G. Galli, D. D. Awschalom, and H. Ohno, Generalized scaling of spin qubit coherence in over 12,000 host materials, *Proceedings of the National Academy of Sciences* **119**, e2121808119 (2022).
- [32] G. Kresse and J. Hafner, Ab initio molecular-dynamics simulation of the liquid-metal–amorphous-semiconductor transition in germanium, *Physical Review B* **49**, 14251 (1994).
- [33] J. P. Perdew, K. Burke, and M. Ernzerhof, Generalized gradient approximation made simple, *Physical review letters* **77**, 3865 (1996).
- [34] International Telecommunication Union (ITU), *Spectral grids for WDM applications: DWDM frequency grid*, ITU-T Recommendation G.694.1 (International Telecommunication Union, Geneva, Switzerland, 2020) accessed 2024-08-15.
- [35] International Telecommunication Union (ITU), *Spectral grids for WDM applications: CWDM wavelength grid*, ITU-T Recommendation G.694.2 (International Telecommunication Union, Geneva, Switzerland, 2020) accessed 2024-08-15.
- [36] A. Dréau, A. Tchebotareva, A. E. Mahdaoui, C. Bonato, and R. Hanson, Quantum frequency conversion of single photons from a nitrogen-vacancy center in diamond to telecommunication wavelengths, *Physical review applied* **9**, 064031 (2018).
- [37] J. Heyd, G. E. Scuseria, and M. Ernzerhof, Hybrid functionals based on a screened coulomb potential, *The Journal of chemical physics* **118**, 8207 (2003).
- [38] W. Wesch, E. Wendler, G. Götz, and N. Kekelidse, Defect production during ion implantation of various a iii bv semiconductors, *Journal of applied physics* **65**, 519 (1989).
- [39] M. Horiki, S. Arai, Y. Satoh, and M. Kiritani, Identification of the nature of small point defect clusters in neutron irradiated fe–16ni–15cr by means of electron irradiation, *Journal of nuclear materials* **255**, 165 (1998).
- [40] R. J. Olsen, K. Jin, C. Lu, L. K. Beland, L. Wang, H. Bei, E. D. Specht, and B. C. Larson, Investigation of defect clusters in ion-irradiated ni and nico using diffuse x-ray scattering and electron microscopy, *Journal of Nuclear Materials* **469**, 153 (2016).